EFDA–JET–CP(10)08/23

M.-L. Mayoral, V. Bobkov, L. Colas, M. Goniche, J. Hosea, J.G. Kwak,
R. Pinsker, S. Moriyama, S. Wukitch, F.W. Baity,
S. Carpentier-Chouchana, A. Czarnecka, A. Ekedahl, G. Hanson,
P. Jacquet, P. Lamalle, I. Monakhov, M. Murakami, A. Nagy,
M. Nightingale, J.-M. Noterdaeme, J. Ongena, P.M. Ryan,
M. Vrancken, J.R. Wilson,
and EFDA –JET contributors*, ASDEX Upgrade team and the ITPA "Integrated
Operation Scenarios" members and experts.

On Maximizing the ICRF Antenna Loading for ITER Plasmas

On Maximizing the ICRF Antenna Loading for ITER Plasmas

M.-L. Mayoral [a], V. Bobkov [b], L. Colas [c], M. Goniche [c], J. Hosea [d], J.G. Kwak[e], R. Pinsker [f], S. Moriyama [g], S. Wukitch [h], F.W. Baity [i], S. Carpentier-Chouchana [l], A. Czarnecka [j], A. Ekedahl [c], G. Hanson [i], P. Jacquet [a], P. Lamalle [l], I. Monakhov [a], M. Murakami [i], A. Nagy [d], M. Nightingale [a], J.-M. Noterdaeme [b,m], J. Ongena [k], P.M. Ryan [i], M. Vrancken [k], J.R. Wilson [d], and EFDA –JET contributors*, ASDEX Upgrade team and the ITPA "Integrated Operation Scenarios" members and experts.

JET-EFDA, Culham Science Centre, OX14 3DB, Abingdon, UK

[a] EURATOM/CCFE Association, Culham Science Centre, OX14 3DB, Abingdon, UK
[b] Max-Planck-Institut für Plasmaphysik, EURATOM Association, Garching, Germany.
[c] CEA, IRFM, F-13108 Saint-Paul-lez-Durance, France.
[c] Princeton Plasma Physics Laboratory, Princeton, NJ 08543, USA.
[d] Korea Atomic Energy Research Institute, Yuseong, Daejeon 350-600, Republic of Korea.
[e] General Atomics, PO Box 85608, San Diego, CA 92186-5608, USA.
[f] Japan Atomic Energy Agency, 801-1, Mukouyama, Naka, Ibaraki-ken 311-0193, Japan.
[g] MIT Plasma Science and Fusion Center, Cambridge, MA02139, USA.
[i] Oak Ridge National Laboratory, Oak Ridge, TN, USA.
[j] Association Euratom-IPPLM, Hery 23, 01-497 Warsaw, Poland.
[k] Association "EURATOM - Belgian State", ERM-KMS, TEC partners, Brussels, Belgium.
[l] ITER Organization, Route de Vinon sur Verdon, 13115 Saint Paul Lez Durance, France.
[m] EESA Department, UGent, Gent, Belgium.
** See annex of F. Romanelli et al, "Overview of JET Results", (23rd IAEA Fusion Energy Conference, Daejon, Republic of Korea (2010)).*

Preprint of Paper to be submitted for publication in Proceedings of the 23rd IAEA Fusion Energy Conference, Daejon, Republic of Korea (10th October 2010 - 16th October 2010)

ABSTRACT

For any given ICRF antenna design for ITER, the maximum achievable power strongly depends on the density profiles in the SOL. It has been suggested that gas injection can be used to modify the SOL profiles and thus minimize the sensitivity of the ICRF coupling to variations in the density at the edge of the confined plasma. Recently joint experiments coordinated by the ITPA were performed to characterise further this method. An increase in SOL density during gas injection led to improved coupling for all tokamaks in this multi-machine comparison. The effectiveness of using gas injection over a wide range of conditions, as a tool to tailor the edge density in front of the ICRF antennas, is documented for different gas inlet location and plasma configurations. In addition, any deleterious effects on the confinement and interaction with the antenna near-field are investigated.

1. INTRODUCTION

Ion Cyclotron Range of Frequency (ICRF) heating relies on the capability of ICRF antennae to radiate power via the Fast Wave (FW) to the plasma core. However, the density in front of the antennas is generally below the FW cut-off density $n_{e,cut\text{-}off}$ and the FW has to tunnel through an evanescence layer of thickness d, the distance from the antenna current-carrying strap to $n_{e,cut\text{-}off}$ [1]. For a plasma with one ion species, $n_{e,cut\text{-}off}$ can be written as:

i.e. $n_{e,cut\text{-}off}$ typically in the 10^{18} m^{-3} range, depends on the antenna spectrum ($k_{||}$ - parallel wave number), the tokamak geometry ($\varepsilon \cong (R_{ant}-R_0)/R_0$ - inverse aspect ratio), the ICRF heating scenario (ω_c/ω - ratio of the ion cyclotron frequency at the major radius R_0 to the operational frequency) and the ion species (A/Z - ratio of ion mass and charge). To first approximation, the maximum achievable ICRF power, can be written as $P_{max}= V^2_{max} R_c / 2Z_c^2$, where V_{max} is the peak maximum voltage on the antenna structure, Z_c is the transmission line characteristic impedance and R_c represents here the antenna loading, referred also as the coupling resistance. The value of R_c is determined by the plasma surface impedance at the boundary of the propagation layer that is sensitive to the electron density gradient, and by the FW RF field attenuation in the evanescence layer of thickness d. It can be shown [2] that $R_c \propto \exp(-\alpha \mid k_{//} \mid d)$ where α is a tunnelling factor that depends on the density gradient at the cut-off. So, R and P_{max}, for a given V_{max} Z_c, and $k_{//}$, are strongly linked to the scrape-off-layer (SOL) density profiles. For ITER, the prediction of the plasma profiles (density and temperature) in the far SOL is still subject to large uncertainties and depends on assumptions regarding the nature of the edge cross-field transport [3]. Recent simulations showed that the two ITER ICRF antennas [4] will couple the minimum required 20 MW in the ITER 15 MA inductive DT scenario but also that the maximum achievable power can vary significantly with different edge assumptions [5][6][7]. Nevertheless, considering the range of plasma current and Greenwald density fraction, the SOL density condition will vary widely and schemes to actively maintain or maximise

the ICRF coupling deserve further investigation. As different plasma fuelling techniques will influence the SOL density profiles differently, it is reasonable to think that suitable gas injection could be used to control the ICRF coupling in ITER allowing either eased operation at lower operating voltage, or an increase in the ICRF power capabilities. Experiments have then been performed on tokamaks worldwide to use gas injection for such a purpose. The coupling modifications, effect on plasma confinement, optimum location for the injection, and RF sheaths are presented in this paper.

2. EXPERIMENTAL SET-UP

This paper will focus on the most recent results obtained on JET, DIII-D, AUG, and TS. The ICRF system properties and conditions of the experiments are summarised in Table 1. Top views of the fours tokamaks are represented on FIG.1. in order to visualize easily the ICRF antenna positions relative to the gas injection inlets. For ITER assuming a DT plasma at 5.3T, typical cut-off densities will be 1 to 4.4 10^{18} m^{-3} depending on the antenna phasing [6]. Using the density profiles described in [7] for the 15MA inductive ITER scenario (refered as scenario 2) and with two SOL assumption for the outward pinch and a wall-separatrix distance of 17 cm, the distance between the antennae strap and the $n_{e,cut\text{-}off}$ position, can vary between 0 (density at the wall above $n_{e,cut\text{-}off}$) and 12.5 cm.

3. EXPERIMENTAL RESULTS

3.1. COUPLING IMPROVEMENT AND CONFINEMENT

The increase in SOL density during gas injection always led on DIII-D, JET, TS, and AUG to an ICRF coupling improvement with no effect on the ICRF heating efficiency and without reduction of the antenna electrical strength (no unusual arcing). In DIII-D experiments (see FIG. 2. and [12]), an increase up to a factor of 6 of the loading in between Edge Localised Modes (ELMs) was observed when injecting D_2 gas at a rate of 1 10^{22} el/s from a pair of orifices adjacent to the antenna 285/300. The loading between ELMs increased from 0.17 Ohm to about 1 Ohm during gas injection. The changes in antenna loading caused by the injection were well correlated with changes in the D_α recycling light viewed by photodiodes - higher loading between ELMs during the injection is correlated with higher $D\alpha$ baseline levels, which in turn indicate higher far SOL density and decreased wave evanescence. Gas injection also increases the ELM frequency, from ~ 38 Hz before the puff to ~100 Hz (somewhat aperiodic ELMs) during the puff. As a result of the reduced edge transport barrier and pedestal height, the global confinement factor H98(y,2) decreased by ~20%. On JET, the coupling increase/confinement decrease vs. gas injection level was found to depend strongly on the plasma configuration used. During experiments reported earlier [10], a very strong, up to 280% (averaged over antennas A, B and D) coupling improvement was observed when injecting 1.8 10^{22} el/s in conditions of strong recycling and high SOL densities typical to the so-called "ITER-like configuration". In the new set of experiments and for the shape referred as "V5 configuration" (filled squared symbol on FIG. 4.), the coupling could be increased by ~ 57% (averaged over 4 antennas) injecting 1.08 10^{22}el/s from GIM6. In that case the confinement was decreased by ~ 15%. In the

HT3 configuration (open triangle symbol on FIG. 4.), that has a higher pumping, the coupling could also be increased by gas puff. Unfortunately, no reference without gas injection exists for this configuration. Nevertheless, an increase from, for example 1.02 to 2.26 10^{22} el/s injection rate from GIM6 gave an overall coupling improvement of 48% (averaged over 4 antennas) which is sligthly lower than the improvement in the V5 configuration. Also, at gas injection rate of ~ 1 10^{22} el/s, the coupling was still much lower than in the V5 configuration. This could be due to a higher averaged cut-off density – antenna distance, firstly because of a lower edge density and secondly because the separatrix is far-away from the antenna upper-half compare to the V5 configuration (see FIG. 3.). At the moment, the uncertainties on the density profiles available and hence cut-off density position do not allow firmer conclusions. Finally, the pulses in the HT3 configuration were prone to Neoclassical Tearing Modes (NTMs) that strongly degraded the confinement. On FIG. 4., only the pulses without NTMs have been kept and although not enough points are available to determine a conclusion on the coupling improvement vs. confinement loss vs. gas injection, one can clearly see that in the HT3 configuration the H98(y,2) factor for a gas injection level of ~ 1 10^{22} el/s is still ~ 1 which is ~ 10% higher than for the V5 configuration with the same gas injected. This different response to fuelling can be attributed to the higher plasma triangularity of the HT3 configuration and related higher pedestal pressure as previously reported in [17].

3.2. COUPLING IMPROVEMENT VERSUS GAS LOCATION

On DIII-D, for the pulse represented FIG. 2., though the gas injection location in this case was local to, and magnetically connected to only one of the two antenna arrays used, the loading on the other antenna was also significantly increased by the puffing, indicating that the effect was not primarily localized to the puffing orifices, but due to a more global increase in far-SOL density.

On JET, different results were observed depending of the plasma configuration used. In previous experiments using the ITER-like plasma configuration [10] a larger coupling improvement was obtained for gas injection from the main chamber, compared to injection from the divertor valves and an influence of the gas inlet locations and proximity to the antennas was also observed. In 2009, using the HT3 configuration that has a similar triangularity but different strike point position, the coupling improvement obtained injecting gas from GIM12 was found to be very similar to that obtained using inlet in the main chamber (see FIG. 4.). Furthermore, when using gas inlet on the top of the machine (GIM5, 8 or 7), no clear higher increase in the coupling of the antennas magnetically connected to the gas inlets was observed, pointing towards a global SOL density increase. The only observed trend being a highest coupling improvement on antenna B for high level of gas injected from the GIM6 pipe that is the nearest to this antenna.

FIG. 5. compares two TS pulses, differing only by the gas injection scheme. In reference pulse TS43025 (black data) the whole fuelling was performed by valve V7, not connected to the ICRF antenna Q5, and feed-back controlled to maintain a prescribed value of line integrated density 4.65 $10^{19}m^{-2}$. Over the pulse the plasma was moved radially away from the antenna. In TS43027 (red

data) a given amount of 1.4Pa.m^3/s (~0.74 10^{21} el/s) was fed through the poloidally distributed valve V9, located toroidally ~5m from antenna Q5 and connected magnetically to the launcher (see FIG. 1). The (small) complement was feed-back controlled from V7 in order to maintain the same core density as in the reference pulse, thus preserving the same recycling. Both valves exhibited similar fuelling efficiencies, so that the total amount of injected gas was similar. As represented on the bottom part of the figure, the coupling of antenna Q5 was similar in both cases and decreased as expected with the separatrix –limiter distance. The surface temperature on the antenna front face, monitored by IR thermography, was also found unchanged. Comparing TS43027 with another pulse at higher target nl and same V7 contribution shows that increasing the total amount of injected gas from V7+V9 by 5% could improve the coupling resistance by up to 10% FIG. 6. AUG – Dependance of the antenna 1 and 4 coupling on the limiter-separatrix distance and for different D2 gas injection location (see FIG.1).

FIG. 6. illustrates the results obtained on AUG, with the coupling resistance of antennas 1 and 4, plotted as a function of the separatrix-antenna limiter distance, for different gas inlet valves, all in the midplane, and two D_2 gas levels [13]. Firstly, as expected, the coupling resistance decreased exponentially with the plasma-antenna distance, consistent with the fact that the cut-off layer moves away from the antenna, and in line with previous ICRF antenna coupling characterization [14]. Secondly, the coupling resistance increased when increasing the level of injected gas (5 10^{21}el/s for the open symbols and ~ 9.5 10^{21} el/s for the filled symbols). Finally, for a given level of injected gas, using gas valves located close to the antenna led to an enhancement of the coupling increase. For antenna 4 (bottom figure), the coupling is significantly higher when injecting gas from the ICR valve (triangle symbols), and similarly the antenna 1 coupling (top figure) benefits more from injecting gas from A1 (squared symbols). From this set of experiments, it could be concluded that although the coupling of the four antennas was improved when injecting gas, indicating a global increase of the SOL density, below a certain distance between the gas injection point and the antenna, the coupling increase became sensitive to the proximity of the valve. Finally, a higher neutral pressure near the antenna 4 was also measured for gas injection at proximity of this antenna. Nevertheless, no firm conclusion could be drawn on the physical mechanism leading to the local density profile modification observed with injection gas near the antenna and several mechanisms are under consideration: neutral ionization by plasma electron impact or by RF $E_{//}$ fields [18], local SOL modification due to E×B drift velocity generated by the RF sheath potential gradient [19], local transport modification (see for example [20]).

3.3. EFFECT OF GAS PUFF ON RF SHEATHS

Finally, the effect of gas injection on non-linear RF waves - edge interaction [21] should not be neglected as it was demonstrated that local parallel heat fluxes due to RF sheaths rectification can lead to significant heat loads on the ICRF antenna frame [22][23]. These fluxes being directly

proportional to the electron density, optimal ICRF operation in ITER might results from a trade-off between reasonable coupling and tolerable heat loads. In TS, (see previous section) when the total amount of injected gas from V7+V9 was increased by 5% and the coupling by up to 10%, more intense hot spots on the antenna structure were observed. Another known effect from RF sheaths is the enhanced sputtering by ions accelerated in the sheath potential. Interestingly, recent analysis [24] of past JET experiments aiming at improving the ICRF coupling with gas injection [19] have shown that the Ni concentration that generally increases during ICRF operation was significantly decreased during gas injection. The reduction of the Ni content with gas puffing was attributed to a change in temperature and density modifications in flow and transport, or to a change in the impurity energy in the SOL and hence sputtering yield. Similar results were also observed on AUG where the W sputtering yield was found to decrease for higher gas puff [25].

4. SUMMARY AND OUTLOOK

In the past years, experiments have been performed in the frame of the ITPA task 5.2 of the Integrated Operation Scenario group in order to investigate the effect of gas injection on the SOL density and linked ICRF coupling in view of ensuring maximum performance of the ITER ICRF system on a broad range of conditions. The results obtained confirmed that gas injection, generally used to fuel the plasma, could also be used to modify the far SOL density and hence increase the ICRF coupling and the maximum achievable coupled power that is directly proportionnal to the coupling. The effect of the location of gas orifices was also investigated and although gas injection from divertor, top or midplane led to a global modification of the SOL density profiles significant enough to improve the ICRF coupling, it was also shown that an injection near the antennas could lead to an additional ICRF coupling improvement for the same amount of gas injected. There are nevertheless, two possible drawbacks to this coupling improvement method. Firstly, it affects (differently depending on the plasma configuration pumping and recycling properties) the plasma pedestal and hence the bulk plasma confinement properties; note that the disavantages associated with such a decrease compared to the advantages of a potential increase in the power imput to the plasmas centre was not yet investigated nor quantified. Secondly, higher density in front of the ICRF antennas will lead to higher RF sheaths-related heat loads. A possible suggestion for ITER, in order to increase further its ICRF system performance, would be to use gas injection preferably locally, controlled in real-time to optimise the required amount of gas ensuring that the requested coupling is reached while controlling any deleterious effects. It is also important to emphasise the importance of having measurements of the far SOL density profiles in front of the ICRF antennas, for ITER but also for present-day machines.

In the meantime, effort should be put on developing the modelling of the experiment described in this paper i.e. development of edge modelling codes (EDGE2D, B2-EIRENE (SOLPS)) to take into account large antenna-limiter distances, inclusion of possible ionisation due to ICRF, 3D neutral gas modelling injection and modelling of RF sheaths and related heat loads. Interestingly for ITER,

new far SOL density profiles have been recently produced as the ITER thermal load specifications defined in [3] have been revised [26] [27] on the basis of the most up-to-date 3D First Wall geometry and on the new reference magnetic equilibrium defined for the Q_{DT} = 10 burning plasma. These new plasma specifications are defined for "low" and "high" density conditions (as for the previous ones - [3]), in keeping with the range of temperatures and densities expected in the ITER SOL according to B2-EIRENE (SOLPS) simulations and direct empirical extrapolation of experimental data from today's tokamaks. It would be advisable to use these latest profiles as input for TOPICA simulations in order to have for this crucial scenario, and up-to-date ICRF power prediction range.

Finally in a near future, experiments are planned on AUG in order to investigate the physical mechanism behind the enhanced coupling increase with gas locally injected. In 2010, experiments will be performed on KSTAR to document the effect of gas injection on the ICRF antenna [28] coupling and installation of an additional gas puff near the ICRF antenna is planned in 2011. The coupling behavior of the C-mod ICRF system [29] with gas injection should also be studied after the installation of a new reflectometer end 2010. Experiments have been proposed for the 2010 TS program, using a new reflectometer between the V9 valve and the Q5 antenna and D_α spectroscopy viewing directly the Q5 antenna. On JET, a proposal to be considered for the 2012 onwards program has been put forward foccusing on the real-time control of gas injection and maximisation of ICRF power in H-mode.

ACKNOWLEDGMENTS

This work, part-funded by the European Communities under the contract of Association between EURATOM and CCFE and EURATOM and CEA, was carried out within the framework of the European Fusion Development Agreement. The views and opinions expressed herein do not necessarily reflect those of the European Commission. This work was also part-funded by the RCUK Energy Programme under grant EP/G003955 and supported in part by the US Department of Energy under DE-FC02-04ER54698, DE-AC02-09CH11466, and DE-AC05-00OR22725.

REFERENCES

[1] STIX, T., 1992 "Waves in Plasmas", AIP Press, ISBN 0-88318-859-7.

[2] BILATO, R., et al., Nuclear Fusion **45** (2005) L5-L7.

[3] LOARTE, A., et al., Fusion Energy Conference 2008 (Proc. 22nd Int. Conf. Geneva, 2008) IT/P6-13 (http://www-pub.iaea.org/MTCD/Meetings/fec2008pp.asp).

[4] LAMALLE P., et al., 18th Topical Conf. on RF power in Plasmas, AIP Conf. Proc. 1187 (2009), p**265**.

[5] MAGGIORA R., et al., 17th Topical Conference on RF power in Plasmas, AIP Conference Proc. 933 (2007), **p171**.

[6] MESSIAEN A., et al., Nuclear Fusion **50** (2010) 025026.

[7] NIGHTINGALE, M., et al., 18th Topical Conference on RF power in Plasmas, AIP Conf. Proc. 1187 (2009), p**213**.
[8] KAYE, A. et al., Fusion Engineering And Design **24** (1994).
[9] MAYORAL, M.-L., et al.36th EPS Conference on Plasma Physics Sofia,, 2009 ECA Vol.33E, O-4.048 (2009).
[10] MAYORAL, M.-L, et al., 17th Topical Conference on RF power in Plasmas, AIP Conf. Proc. 933 (2007), p**55**.
[11] PINSKER, R.I. et al., Fusion Science Technology **48**, 1238 (2005).
[12] PINSKER, R.I. et al., 37th EPS Conference on Plasma Physics Dublin, Ireland, 21-25 June 2010, (http://ocs.ciemat.es/EPS2010PAP/pdf/O4.124.pdf).
[13] JACQUET, P. , et al., CCFE report, CD/ICRH/RF/0053 on EFDA task WP09-HCD-02/04/UKAEA (2010).
[14] BOBKOV, Vl.V., et al., Nuclear Fusion **46** (2006) S469–S475.
[15] BEAUMONT, B., et al., Proc. 15th SOFT (Utrecht, The Netherlands, 1988), p **503.**
[16] COLAS, L., et al, Nucl. Fusion **46** (2006) S500–S513.
[17] SARTORI R et al., Fusion Energy Conference 2004 (Proc. 20th Int. Conf. Vilamoura, 2004) EX/6-3, (http://www-naweb.iaea.org/napc/physics/fec/fec2004/datasets/index.html).
[18] LYSSOIVAN, A.I. et al, Journal of Nuclear Materials **337-339** (2005) 456-460.
[19] BECOULET, M., et al., Physics Plasmas, Vol. 9, No. 6, June 2002.
[20] MATTHEWS G F, et al., Plasma Physics and Controlled Fusion **44** 689–699, (2002).
[21] MYRA, J.R, et al., Nuclear Fusion **46** (2006) S455-S468.
[22] COLAS, L., et al., 18th Topical Conference on RF power in Plasmas, AIP Conf. Proc. 1187 (2009), p**133**.
[23] JACQUET, P., EXW/P7-32, this conference.
[24] CZARNECKA, A., et al., 37th EPS Conference on Plasma Phys. Dublin, Ireland, 21-25 June 2010.
[25] BOBKOV, Vl.V., et al., Nuclear Fusion **50** 035004, (2010).
[26] PITTS, R. A., et al., 19th International PSI Conference, San Diego (US), 2010.
[27] CARPENTIER, S., et al., 19th International PSI Conference, San Diego (US), 2010.
[28] Y.D. BAE, Y.D, et al., Fusion Engineering and Design **82** (2007) 765–770.
[29] PARISOT, A., et al., Plasma Physics and Controllled Fusion **46** (2004) 1781–1792.

	JET	**DIII-D**	**AUG**	**TORE SUPRA**
ICRF antenna	4 * 4 straps A2 antennas (A, B, C, D) with: - C and D paired by external conjugate T (ECT) junction - A and B paired by 3dB hybrid coupler - 1 * 8 straps ITER-like antenna – *Not used here*.	3 * 4 straps antennas (285/300, 0, 180)	4 * 2 straps antennas (1, 2, 3, 4) with: antennas 1 and 3 (and 2 and 4) paired by 3dB hybrid couplers. *Note that the usual pairing is 1-2 and 3-4*	3 * 2 straps antennas (Q1, Q2, Q5)
Ref.	[8][9][10]	[11] [12]	[13] [14]	[15][16]
f_{ICRF} (MHz)	23-57 (42 in this paper)	30-120 (60 and 90 in this paper)	30-60 (30 in this paper)	40-80 Minority heating (H)D
Heating scheme	Minority heating (H)D	ELD/TTMP electron heating	Minority heating (H)D	Minority heating (H)D
$\|k_{//,max}\|$ (m^{-1})	6.6 ($\Leftrightarrow\pi$ phasing)	6 (285/300) & 7.4 (0,180) ($\Leftrightarrow \pi/2$ phasing)	8 ($\Leftrightarrow\pi$ phasing)	13 ($\Leftrightarrow\pi$ phasing)
$n_{e,cut-off}$ (m^{-3})	2 10^{18}	1 10^{18}	5 10^{18}	9 10^{18}
$d_{strap-limiter}$ (cm)	5.1	5.7 (285/300) & 4.1 (0)	3.9	5.5
$d_{limiter-LCFS}$ (cm)	10-14	2-12.5	4.5-10.5	1-8.5
B_T (T)	2.6	1.3-2.1	2	3.8
NBI power (MW)	14-17	3-14	none	none
D_2 injection (10^{21} el/s)	0-24	0 - 15	0.5 – 10	0.8
Confine--ment mode	ELMy H-mode	ELMy H-mode	L-mode, near H-mode	L-mode
Pumping	Cryopump in the lower divertor	Cryopump at the upper & lower divertor	Cryopump in the lower divertor	Pumped limiter

Table 1. Overview of the parameters used in the experiments described in this paper

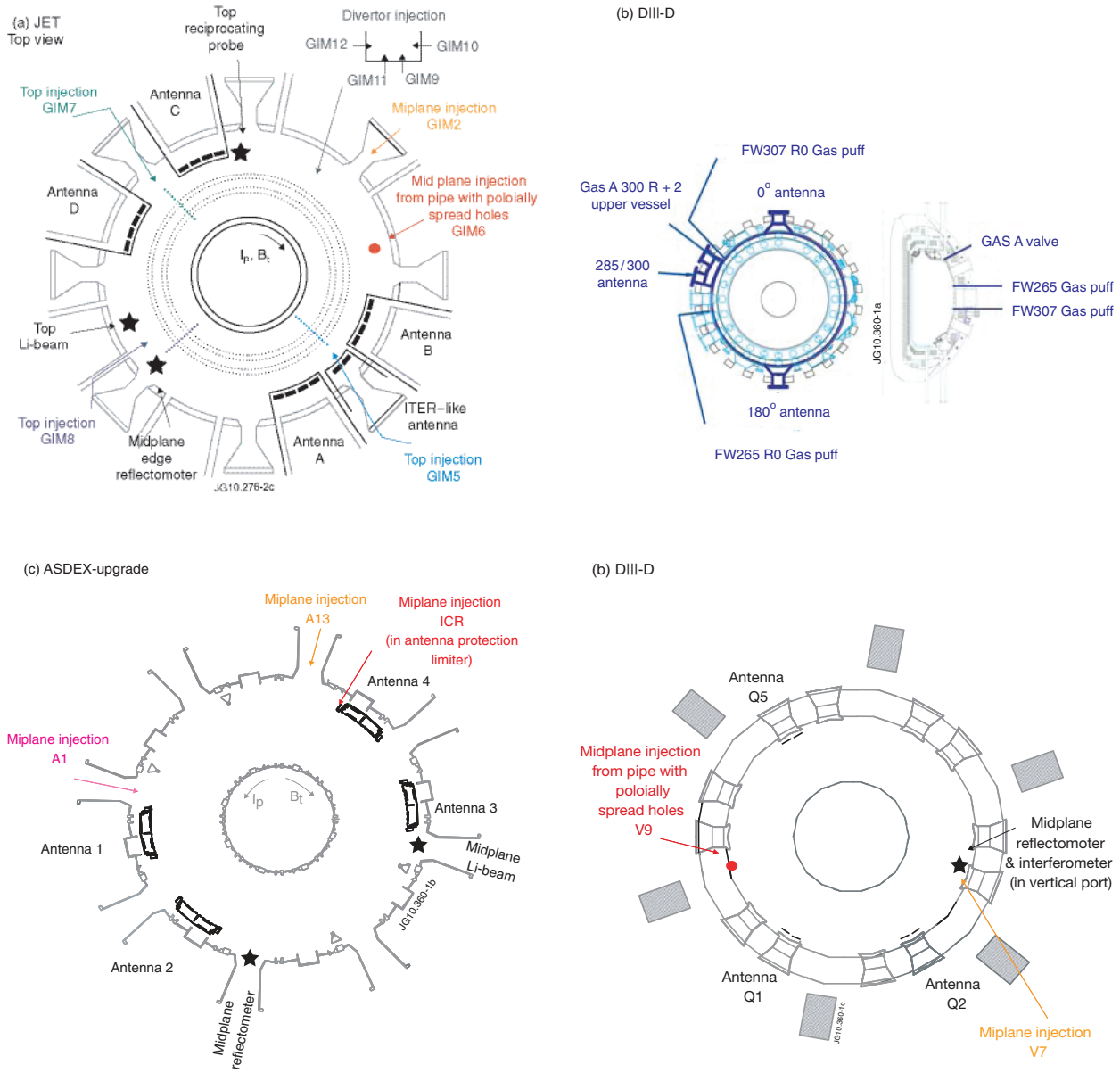

Figure. 1. Top view of (a) JET, (b) DIII-D, (c) AUG and (d) Tore Supra. The ICRF antennas, gas injection locations and relevant edge density diagnostic position are represented.

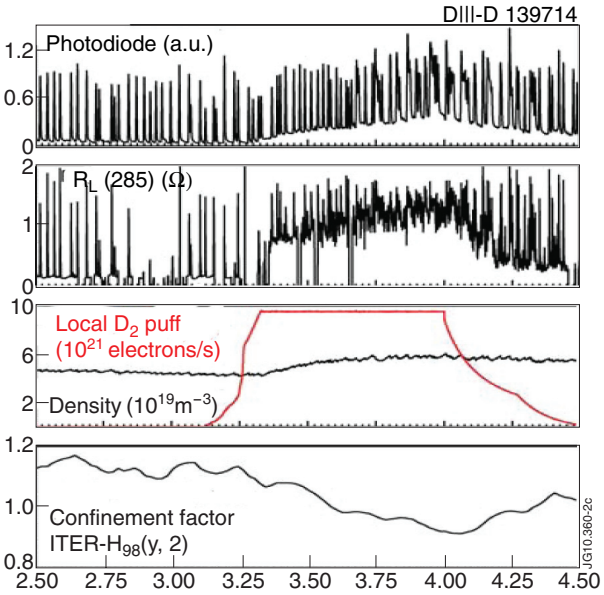

Figure. 2. DIII-D – Time evolution of ELMs, antenna 285/300 coupling, D2 injection rate, central electron density, confinement factor.

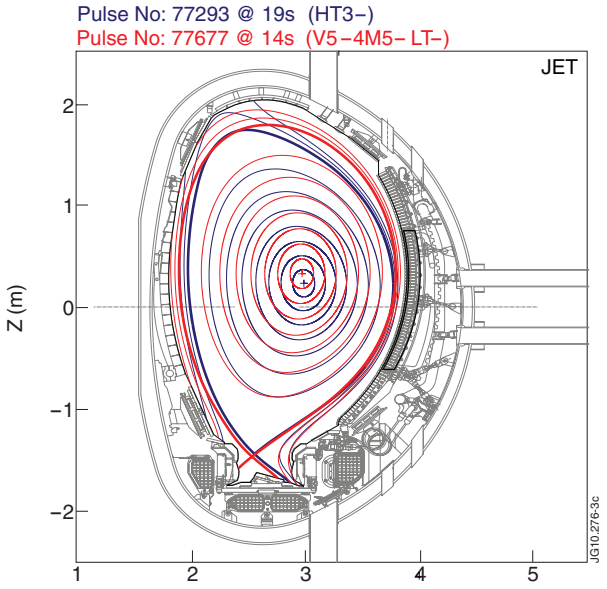

Figure. 3. JET - Comparison of the plasma shape referred as HT3 and V5 in FIG. 4. The separatrix-strap distance at the midplane is similar and around 17 cm.

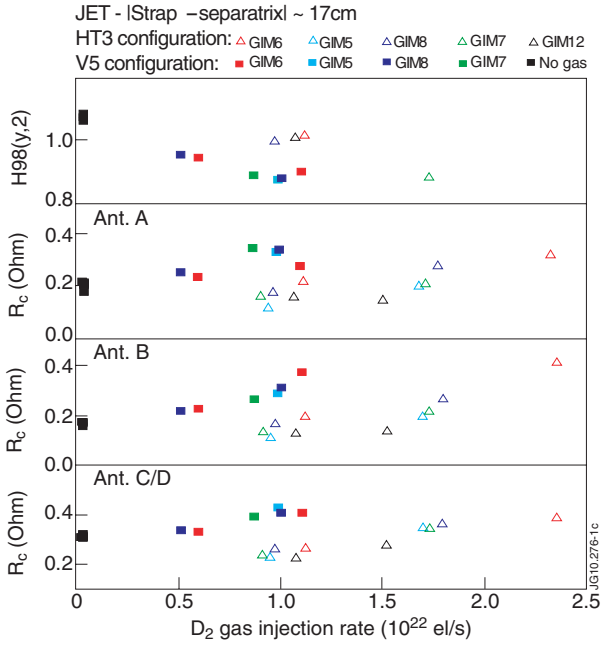

Figure. 4. JET - Evolution of H98(y,2), antenna A, B and C/D coupling in between ELMs function of D2 injection rate for different gas inlet (see FIG. 1.) and two plasma configurations (see FIG. 3.). In the ECT layout, Rc for C and D cannot be decoupled. To maintain the H level, 0.1 10^{21} el/s from GIM11 and 0.03 1021 el/s from GIM9, respectively for HT3 and V5, were injected throughout the pulses.

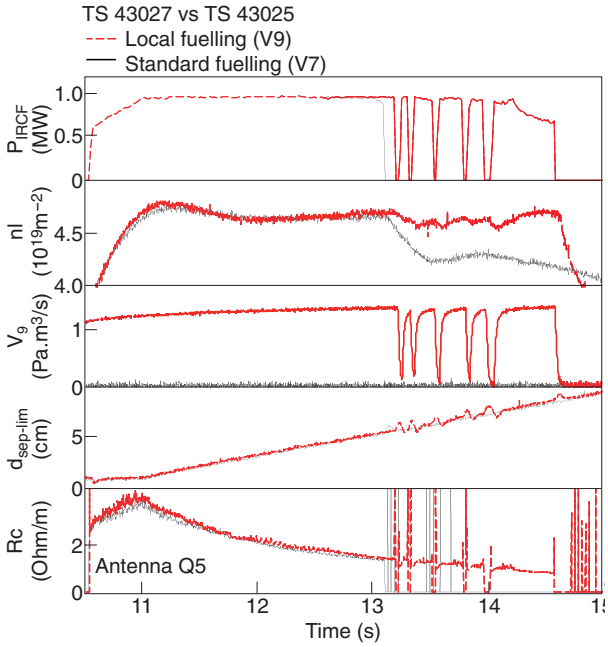

Figure. 5. TS - Time evolution of the ICRF power, line averaged density, D2 injection from valve 9 (with 1.4 Pa.m3/s ~ 0.74 10^{21} el/s), limiter- separatrix distance and antenna Q5 coupling for a pulse with injection from V9 (magnetically connected to Q5) and from V7.

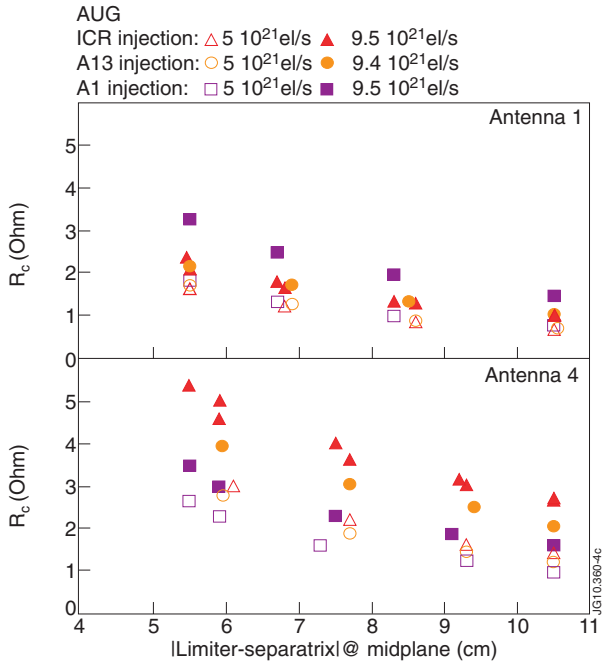

Figure. 6. AUG – Dependance of the antenna 1 and 4 coupling on the limiter-separatrix distance and for different D_2 gas injection location (see FIG.1).